

## Short-Range Ensemble Forecasting of Explosive Australian East Coast Cyclogenesis

LANCE M. LESLIE

*School of Mathematics, University of New South Wales, Sydney, Australia*

MILTON S. SPEER

*Bureau of Meteorology, Sydney, Australia*

(Manuscript received 15 November 1996, in final form 17 March 1998)

### ABSTRACT

Explosive cyclogenesis occurs on average once a year over the coast of New South Wales (NSW), Australia. Known locally as east coast lows, these storms are characterized by very strong winds and heavy rain. Intensity, size, proximity to the coast, and speed of movement of the cyclone are important in their impact on coastal NSW, especially Sydney. Predicting the location of the system, the maximum sustained wind speeds, and the rainfall totals all are operational forecasting challenges. Warnings are issued when predictions exceed threshold values. For example, *land gale* forecasts are issued if sustained wind speeds are expected to reach or exceed 34 kt (about  $17 \text{ m s}^{-1}$ ). The east coast low of 30–31 August 1996 featured land gales over the greater Sydney area. No warnings were issued as the forecasters estimated that the wind strength would fall below gale force. In this study, uncertainty in the predictions is estimated and reduced by providing, in addition to the routine single operational numerical weather prediction, a Monte Carlo–based short-range ensemble (SREF) approach. The intention is to improve the forecasts and also to provide valuable statistical information such as sea level pressure probability ellipses and estimates of the variances in the wind and rainfall predictions. For this event, both the unperturbed and ensemble forecasts predicted sustained maximum wind speeds in excess of 40 kt ( $20 \text{ m s}^{-1}$ ) at the official Sydney observation station. However, the SREF provided vital additional information, namely, that over 70% of the forecasts were within one standard deviation (plus or minus 5 kt) of the mean. The SREF guidance therefore strongly supported the prediction of land gales. Moreover, although the ensemble forecast mean slightly underpredicted the rainfall total at Sydney, the forecast spread encompassed the observed 24-h total of 127 mm.

### 1. Introduction

Australian east coast cyclones, particularly the explosive form, are a significant forecasting problem in terms of predicting the location and central pressure of the cyclone, the occurrence of land and ocean gale force winds, the location and amount of rainfall, and the likelihood of associated storm surges. The commonly accepted working definition is that a fully developed Australian east coast cyclone has a closed cyclonic circulation at the surface, it forms in a maritime environment within  $5^\circ$  of the eastern coastline, its center is located between  $20^\circ$  and  $40^\circ\text{S}$  and within  $5^\circ$  of the eastern coastline, it must exhibit some motion parallel to the eastern coastline, and there should be a pressure gradient of at least  $4 \text{ hPa } (C^\circ)^{-1}$  near the center. Defining these characteristics of Australian east coast storms, Hopkins and Holland (1997) studied associated heavy rain days from 1958 to 1992. On a long-term average, Australian east

coast cyclones occur approximately once per annum, mainly during either winter or the transition seasons when the land–sea contrast is greatest and upper-level support is most likely. The east coast low of 30–31 August 1996 cost at least two lives and caused almost \$20 million (Australian dollars) in damage. The cost in recent years from the two previous most destructive east coast cyclones was estimated at \$12 and \$8 million (Australian dollars) in August 1990 and September 1995, respectively. Existing numerical model skill in predicting their formation and subsequent motion is reasonably good. For example, numerical studies almost a decade ago by Leslie et al. (1987) showed that development can be predicted provided the synoptic-scale processes are present in the initial conditions, but the degree of intensification depends critically on the adequacy of the representation of mesoscale processes. In particular in that study, cumulus convection and surface fluxes were found to be necessary for the intensification process. More recent studies have revealed similar success (see, e.g., Hess 1990; McInnes and Hess 1992). However, central pressures generally are forecast too high because the systems frequently have a core of

---

Corresponding author address: Milton S. Speer, Bureau of Meteorology, P.O. Box 413, Darlinghurst, NSW 2010, Australia.  
E-mail: m.speer@bom.gov.au

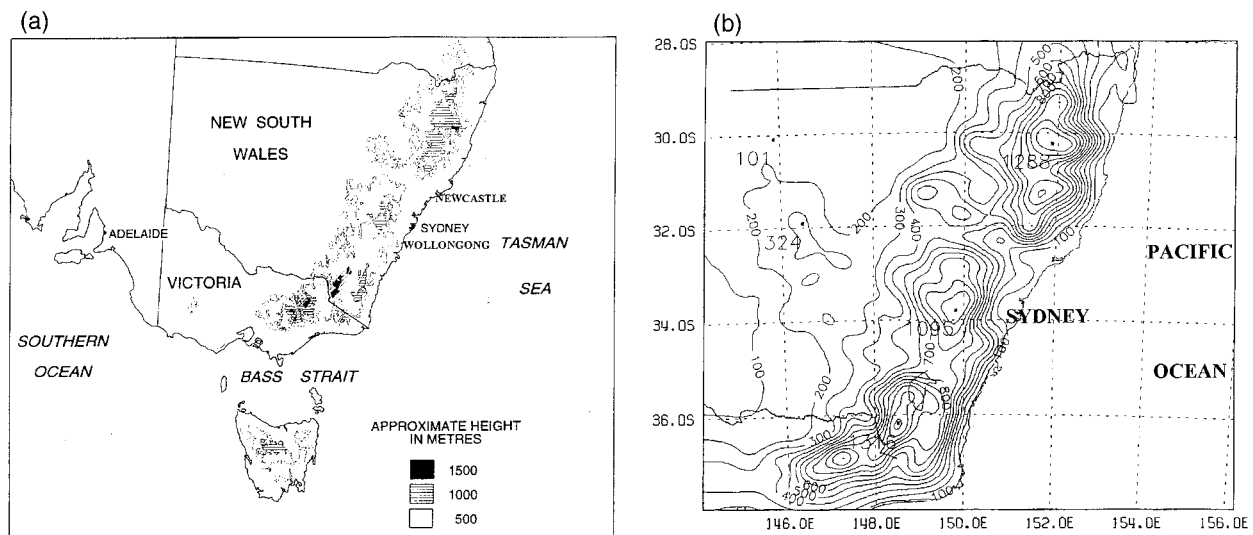


FIG. 1. (a) Map of southeastern Australia showing topography (m) and some locations mentioned in the text. (b) HLAM domain at 15 km (64 × 73 grid points, 25 levels) horizontal resolution, showing topographical contours (m).

strong winds that were not well resolved by existing operational model resolutions, such as the Bureau of Meteorology's (BoM) operational Limited Area Prediction System (LAPS). These resolutions were 75 km and 19 vertical levels for the entire Australian region (Puri et al. 1996). Despite the above-mentioned success in predicting east coast cyclogenesis, there is considerable potential for reducing forecast position and intensity errors. The motivation for this study was the fact that on 30 August 1996 there were signs from the numerical guidance provided by LAPS that explosive east coast cyclogenesis would occur somewhere off the coast. However, uncertainty still remained with the forecasters as to the likely location of the center, especially the proximity to the coast and the intensity of the storm. Given that the area threatened included Australia's most densely populated region, the central coast of New South Wales (NSW), which contains the cities of Sydney, Newcastle, and Wollongong (see Fig. 1a), there is a demand for forecasts containing probabilistic information to supplement that provided by a single forecast. As has been well documented, the problem with a single

forecast is that the forecast uncertainty is not conveyed to the user and, as Doswell (1996) points out, if a forecast containing probabilistic information (e.g., an ensemble mean and measure of forecast spread) is provided, then the responsibility for decision making is rightly with the user rather than with the forecaster as in the categorical single forecast approach. As it turned out, the main difficulty with this event was very specific: whether or not to forecast land gales, that is, wind speeds greater than 34 kt or 17.5 m s<sup>-1</sup>.

In this study we attempt to resolve the uncertainty in predicting the location and intensity of the center employing a Monte Carlo short-range ensemble forecasting (SREF) mode comprising a large number (100) of perturbed initial states and with a simulated real-time model run at 15-km horizontal resolution over southeastern Australia. The simulation involved the use only of real-time archived data so it was formally equivalent to a real-time run. This is especially true given that the ensemble run took only about 50% more time than the maximum operational time slot of about 1 h allowed for the real-time regional forecasts. Details of this model are discussed in section 2. The approach is similar to that successfully used by Mullen and Baumhefner (1989, 1994, hereafter referred to as MB89 and MB94, respectively) in their studies of marine cyclogenesis in the United States. Details of the approach adopted here are given in section 2, below. Although the types of cyclogenesis are quite different in detail, they are generically similar. Questions that will be addressed are the value of the ensemble approach in practice in terms of both improved accuracy and the additional time required to run the ensemble. This test case was chosen largely because it provides an almost classic example of Australian east coast cyclogenesis. Although it is well

TABLE 1. Details of the HLAM model.

Model feature	HLAM
Horizontal resolution	15 km
Numerical scheme	Split semi-implicit (high order)
No. of vertical levels	25
Assimilation scheme	6-h cycling
Initialization	Dynamic
Orography	2-min resolution
Boundary layer scheme	Mellor–Yamada, level 2.25
Radiation scheme	Fels–Schwarzkopf
Convective scheme	Kain–Fritsch
Sea surface temperatures	5-day average
Lateral boundary conditions	From LAPS model

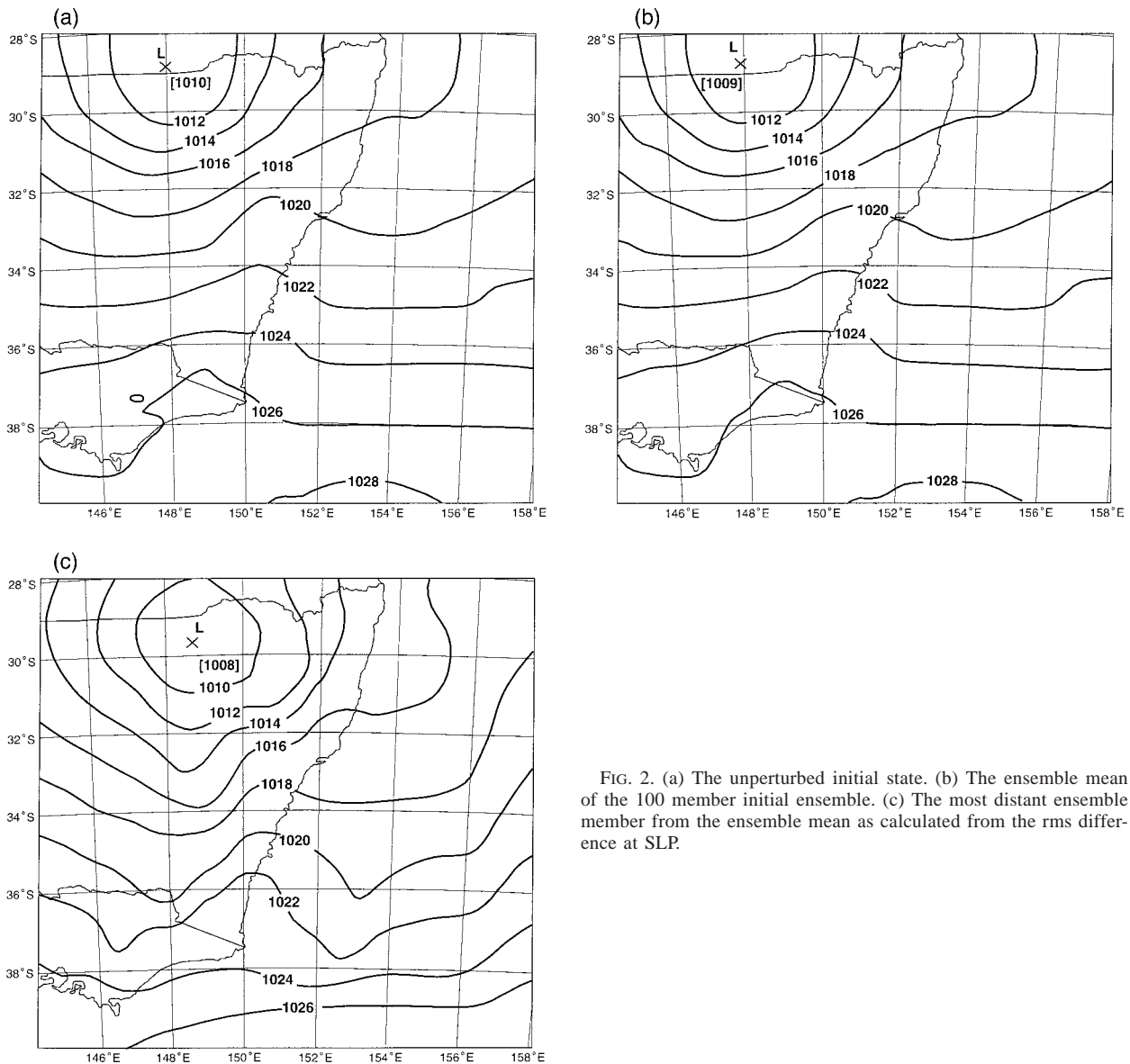


FIG. 2. (a) The unperturbed initial state. (b) The ensemble mean of the 100 member initial ensemble. (c) The most distant ensemble member from the ensemble mean as calculated from the rms difference at SLP.

known that there is large case to case variability in SREF studies, this case was forecast reasonably well by the 75-km operational model given its resolution limitations. A synoptic overview of the east coast low of 30–31 August 1996 is presented in section 3, and the results from the single forecast and SREF are detailed in section 4. It was hoped, therefore, that this case would provide a good test of the ability of the SREF approach especially when applied to a much higher resolution model nested within it. Implications from the results of this study with respect to the relative merits of the single forecast approach versus the ensemble approach are discussed further in section 5.

## 2. Ensemble methodology

Presently, there are three main methods in common use for the creation of ensemble members. The National Centers for Environmental Prediction (NCEP) uses the so-called breeding method (Toth and Kalnay 1993) and the European Center for Medium-Range Weather Forecasts (ECMWF) uses the singular vector decomposition approach (Molteni et al. 1995). We have chosen a third approach, the Monte Carlo procedure, which has also been used successfully (see, e.g., MB89 and MB94) but has suffered in the past from the prohibitive computational cost of generating a sufficiently large ensemble. Questions have rightly been raised about the relative

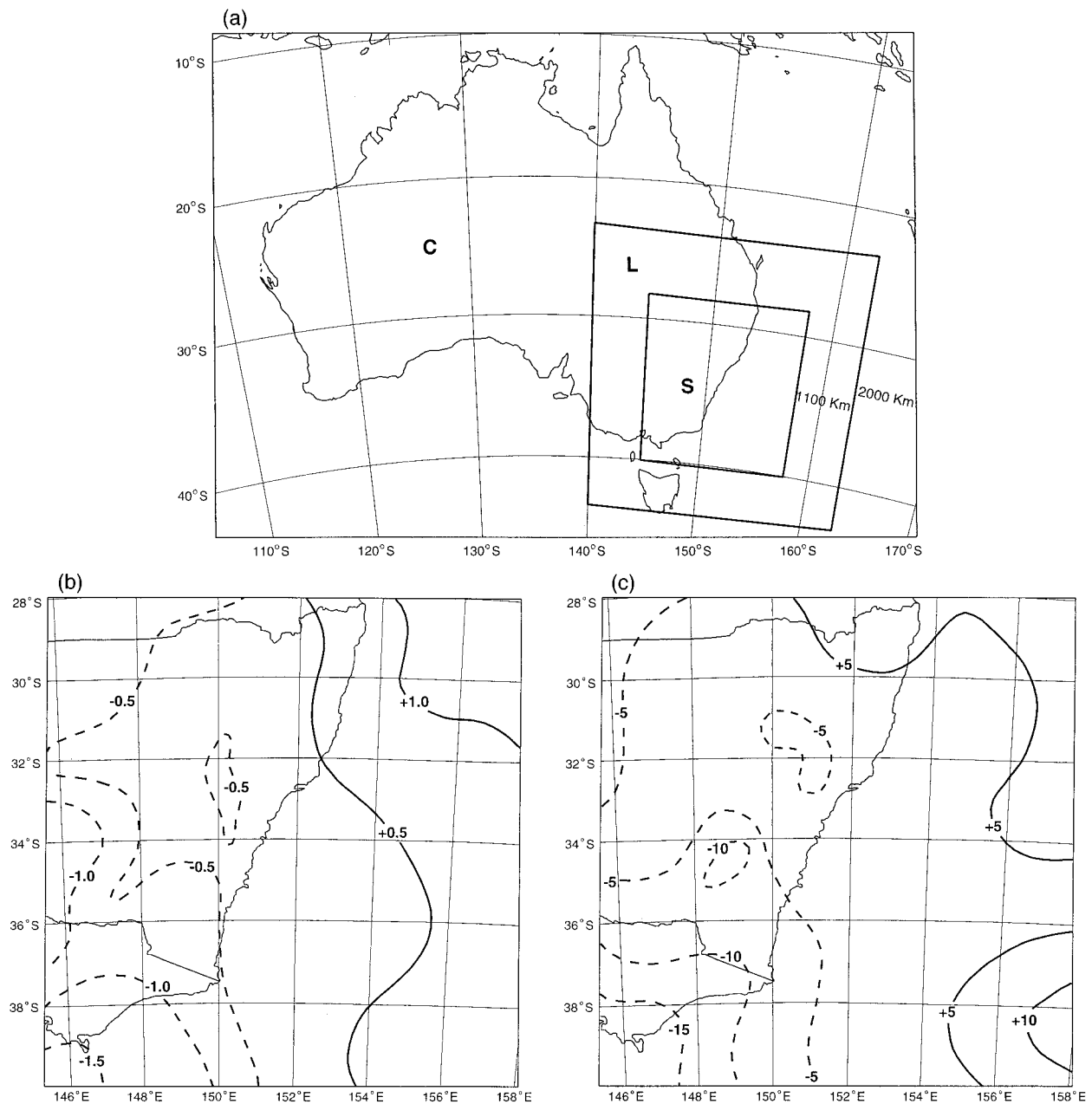


FIG. 3. (a) The coarse mesh model domain C, and the two domains L (large) and S (small) used for testing the sensitivity of the forecasts to the lateral boundary conditions. (b) The 36-h difference between the SLP forecasts (hPa) for the L and S domains, both nested in the coarse mesh model. (c) As in (b) except for 500 hPa.

merits of allocating resources to better single forecast approaches or using degraded resolution models in the SREF approach (Brooks et al. 1995). As will be explained later, this choice was not particularly important here. However, the continued exponential growth in computing power means that it is feasible now to perform large numbers of runs of a high-resolution limited-area model in real time. For example, this has been achieved over an area the size of southeastern Australia using the boundary conditions from the operational

model forecast to nest the limited area model developed jointly by Leslie and Purser (1995). This model is referred to as the High Resolution Limited Area Model (HLAM). Details of the model are summarized in Table 1. The 15-km horizontal resolution domain is shown in Fig. 1b. Initial and boundary conditions were provided from LAPS forecast for the coarse mesh run (75 km), and the 15-km HLAM runs were produced by nesting within the 75-km LAPS model and without varying the boundary conditions for any of the ensemble members.

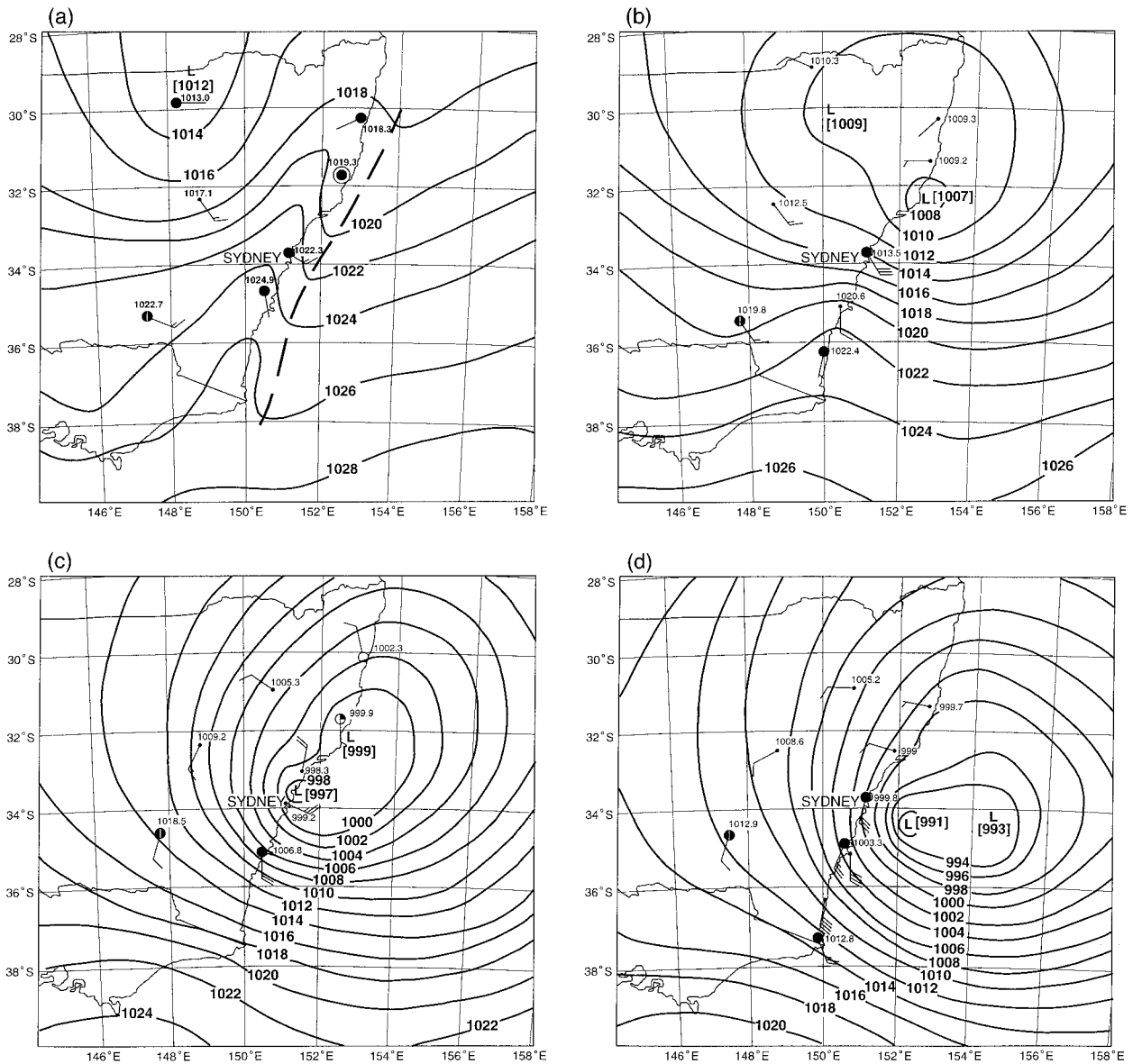


FIG. 4. SLP analyses based on LST observations for (a) 0900 30 August 1996, (b) 2100 30 August 1996, (c) 0900 31 August 1996, and (d) 2100 31 August 1996.

The importance of the boundary conditions will be discussed below in some detail.

*a. Monte Carlo method*

The general procedure for carrying out a Monte Carlo forecast involves the generation of a finite sample of equally likely initial states, advancing each of those states using model equations and the determination of an estimate of the true state at any later time using the sample mean. The uncertainty of the initial state is given by covariances generated by the BoM's operational analysis scheme. As the sample size approaches infinity, the forecast based on the sample mean becomes "best" in

the sense that it is unbiased and possesses minimum variance. From earlier work on turbulence flows (Leith 1974), relative mean square velocity errors were reduced significantly up to a sample as small as 8 or 10 initial states. Larger numbers of initial states are now used in operations, for example, at NCEP and at ECMWF. Although similar to MB89 and MB94, the perturbation methodology adopted has significant differences. Other studies performed by the first author (LML) with tropical cyclones involved perturbing the wind field only, whereas MB89 (p. 2801) perturbed only temperature as the case was a midlatitude event. Australian east coast lows occur in the subtropics, usually between 28° and 38°S (Sydney is at 34°S) so it was decided to apply

random perturbations to both the wind and the temperature. The perturbations were also applied directly to the gridpoint model and not in spectral space as in MB89 and MB94. The size of the perturbation was determined from known analysis error characteristics as discussed below. The boundary conditions supplied by the coarse-resolution model forecasts at 12-h time intervals were not perturbed.

The procedure adopted here for the generation of the ensemble members is, we believe, a very effective one and needs some elaboration. The random perturbations were treated as if they were data and added to the other observational data available. This combination of observations and random noise was then used to generate up to 100 initial analyses for the forecast model using the operational regional data analysis scheme, which is basically a multivariate statistical analysis scheme. This method of generating the ensemble members has great appeal as it not only spatially correlates the perturbations in both the horizontal and vertical via the analysis scheme but it also renders, in the truest sense we are aware of, each member of the initial ensemble as "equally likely." Three initial states are shown in Figs. 2a–c, all of which would be regarded as defining the initial state to within analysis errors. Figure 2a is the unperturbed sea level pressure (SLP) analysis, Fig. 2b is the initial ensemble mean SLP analysis, and Fig. 2c is the perturbed analysis most remote from the ensemble mean in the sense of a simple rms difference. The striking aspect of the initial analysis in this case is its structural simplicity, with basically one shallow major feature, namely, the trough over the central northern part of the chart. Finally, the perturbed initial fields were passed through a diabatic dynamic initialization procedure (Daley 1991, 323), which does little more than filter out spurious gravity waves. The procedure was very effective as the initialized fields were free from high-frequency gravity waves and the forecasts exhibited little or no initial shock.

#### b. Size of initial perturbations

The data density imposes a constraint on the envelope of the amplitude of the perturbations, the envelope being larger over the data-sparse oceans. For this study, the errors for analyzed winds over the Australian region typically are  $7 \text{ m s}^{-1}$ ,  $5 \text{ m s}^{-1}$ , and  $3 \text{ m s}^{-1}$  for the upper, middle, and lower levels (300 hPa, 500 hPa, and 850 hPa), respectively. Analysis temperature errors were  $1.5^\circ\text{C}$  at each of these levels. No attempt was made in this study to test the sensitivity to perturbations of the moisture field. The 100 initial states were generated by adding Gaussian noise at each grid point, constrained within the above-mentioned error limits for the wind and temperature fields, after which each perturbed analysis was initialized using HLAM.

In summary, then, the procedure consisted of generating the 100 model forecasts using HLAM at 15-km

horizontal resolution centered on NSW (Fig. 1b). Initial and boundary conditions were provided by the coarse mesh LAPS model interpolated from 75 km to 15 km. The 15-km horizontal resolution was deliberately chosen for two main reasons: it is considered to be close to the current practically feasible horizontal resolution at which the model will be run locally in real time on the recently acquired BoM computer upgrade; and it does not violate the nonhydrostatic and cumulus parameterization assumptions (Golding and Leslie 1993).

#### c. The impact of lateral boundary conditions

It is well known that there are potential problems associated with lateral boundary conditions in limited-area forecast models, and a recent article by Warner et al. (1997) provides a comprehensive overview of these problems and suggests practical ways in which they can be minimized. In fact, the domain used here was chosen very carefully after experimentation and many years of prior knowledge of the region. However, it still is instructive to look at the error patterns at 36 h for the domain used and also for a domain with the lengths of the sides doubled in each of the horizontal directions. Given that the interest was on the short-range period out to 36 h only, our expectations were that the domain was large enough. The integration domains are shown in Fig. 3a and are labeled C for the Australian region coarse mesh model domain (50-km horizontal resolution), L for the large 15-km resolution domain, and S for the small 15-km resolution domain used for the experiments described in this study. That the smaller domain is large enough, at least for the present event, is confirmed in Figs. 3b and 3c, which show the error fields near the surface and at 500 hPa. Here, the error fields are defined, conventionally, as the difference between the forecasts over domains L and S, both nested in the coarse mesh model and both run at the same resolution of 15 km. The smaller domain shows some evidence of larger errors penetrating the edges of the area of interest but they are quite small, being everywhere less than 2.0 hPa at SLP and less than 20 m at 500 hPa. Not surprisingly they are largest in the southwest corner of the domain. The larger domain was not selected because the additional computational cost was not justified by the relatively minor influence of the boundary conditions. In other regions, for example in the midlatitudes, a larger region might be required but it would be assessed before a final configuration was settled upon.

### 3. The east coast low of 30–31 August 1996

The main interest in this event was the combined effects of heavy rain and strong to gale force winds with extreme gusts of 64 and 53 kt ( $33$  and  $17 \text{ m s}^{-1}$ ) recorded near Wollongong, just to the south of Sydney, and Sydney airport, respectively, after the initial formation of the low just off the coast near Newcastle. Coastal dam-

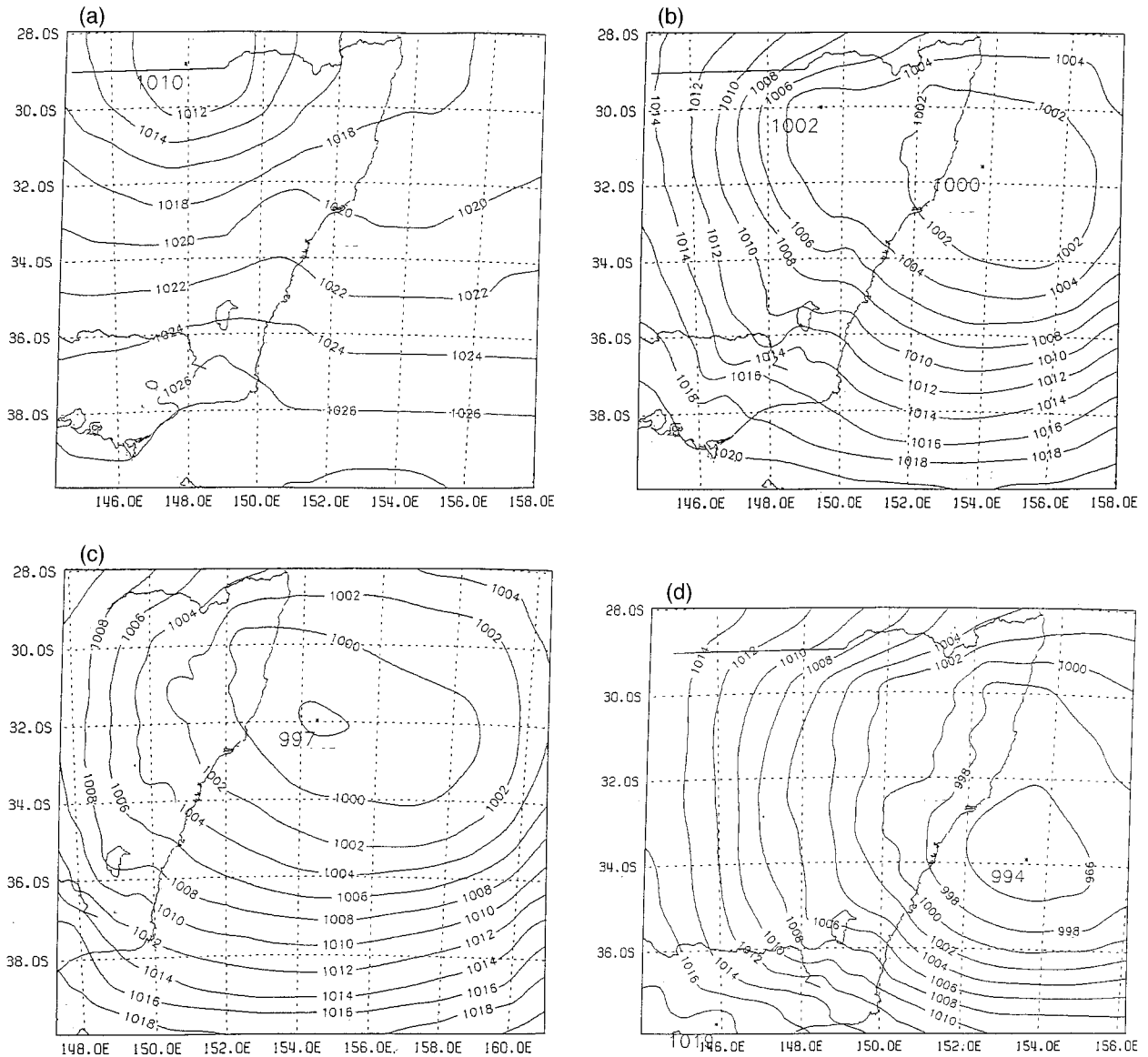


FIG. 5. (a) Initial HLAM SLP analysis valid at 0900 30 August 1996, (b) 12-h HLAM SLP forecast valid at 2100 30 August 1996, (c) 24-h HLAM SLP forecast valid at 0900 31 August 1996, (d) 36-h HLAM SLP forecast valid at 0900 31 August 1996, (e) graph showing hourly modeled and observed SLP pressure at Sydney airport from 0900 30 August 1996 to 0900 31 August 1996, and (f) 36-h HLAM wind forecast at 12 m valid at 2100 31 August 1996.

age from fallen trees was widespread, occurring 80 km on either side of Sydney with some flash flooding reported in the Sydney metropolitan area. At 0900 LST 30 August 1996 a surface low with central pressure of 1012 hPa was located over inland eastern Australia (Fig. 4a). A positively tilted trough was well developed into the upper troposphere and strong temperature gradients there provided baroclinicity. At 500 hPa the trough extended northwest across the Tasman Sea from New Zealand to inland New South Wales where there was a circulation in the apex of the trough. A subtropical jet maximum with speeds reaching 140 kt ( $72 \text{ m s}^{-1}$ ) at 300 hPa was evident farther west between  $30^\circ$  and  $35^\circ$ S

such that the circulation in the trough was situated near the right exit region of the jet maximum as the jet maximum moved around the equatorward side of the trough. As the circulation in the midtroposphere gradually intensified, a surface low started developing just offshore north of Newcastle late on August 30 (Fig. 4b) and intensified in the next 12 h due to the mesoscale factors mentioned in section 1. A very small center formed over the Sydney metropolitan area early on August 31, then moved southeast to be just off the coast at 1500 LST from where it continued its southeast movement together with the first center still east of Newcastle. The central pressure dropped 12 hPa in the 12 h between

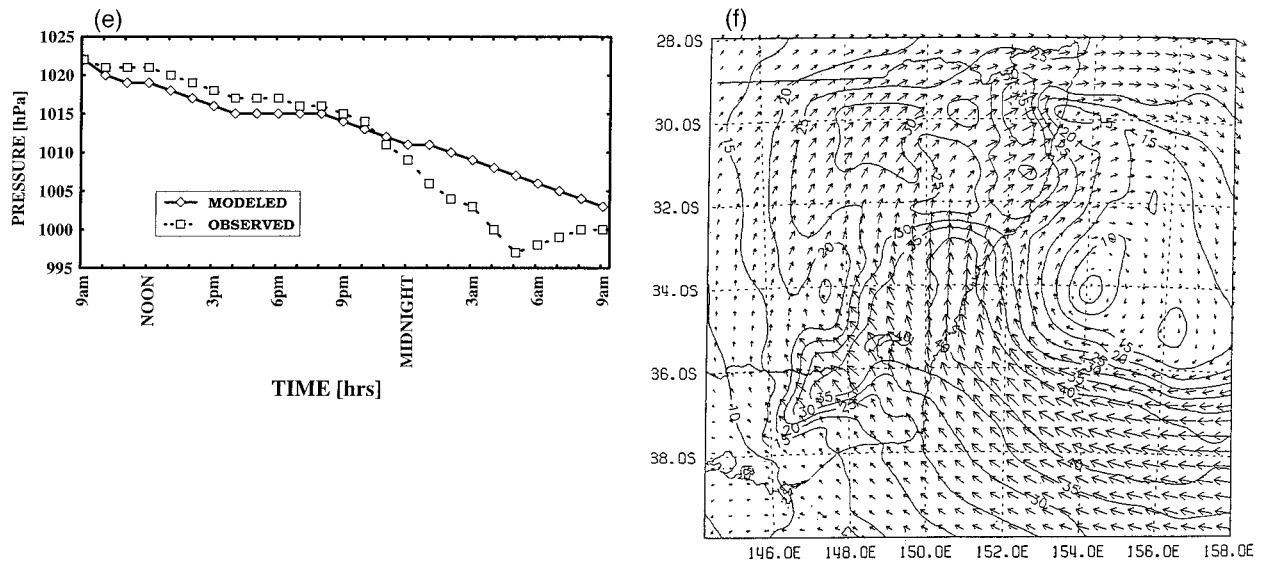


FIG. 5. (Continued)

2100 LST 30 August and 0900 LST 31 August (Fig. 4c). The latitude-corrected pressure drop for the 24 h to 0900 31 August was 1.1 Bergeron (17 hPa uncorrected) so most of the intensification occurred overnight. This exceeds the intensification criterion of 1 Bergeron as defined by Sanders and Gyakum (1980) for maritime “bombs.” The severe wind gusts combined with the antecedent rain a few hours before caused many trees to fall. After 0900 31 August the system, now with the two centers, that is, the one still east of Newcastle and the new small circulation over Sydney, started to move

to the southeast away from the coast, intensifying a further 6 hPa in the 12 h to 2100 31 August (Fig. 4d).

#### 4. Results

##### a. Unperturbed analysis and forecasts

The unperturbed initial SLP field shown in Fig. 5a was generated by HLAM using dynamic initialization on the unperturbed archived numerical analysis interpolated from 75 km to the 15-km grid. It corresponds to the manually generated analysis (Fig. 4a), which is based on observations at 0900 30 August 1996. As such, the manual analysis has more data and exhibits greater structure, especially the trough zone just off the coast. The observed central pressure in the low of 1012 hPa is 2 hPa higher than in the initialized field. Despite the relative smoothness of the numerical initial field near the coast, it plays little role in the cyclogenesis, and the major development, that of the east coast low, is not unduly affected.

At 2100 30 August the 12-h SLP forecast has started to develop a low just off the coast near Newcastle (Fig. 5b), while at the same time maintained the inland center as in the verifying analysis (Fig. 4b). There is a difference of 7 hPa in the low center’s intensity between the analysis and forecast. However, given the lack of observations off the coast, the intensity of the low center could have been greater, and closer to the forecast intensity of 1000 hPa. At 0900 31 August (corresponding to the 24-h forecast), the vortex off the coast had become multicentered with the original vortex (hereafter referred to as **V1**) dramatically intensifying similar to the observed as indicated in the manual analysis (Fig. 4c), but the 24-h SLP forecast (Fig. 5c) did not predict the new, very small center (hereafter referred to as **V2**), on

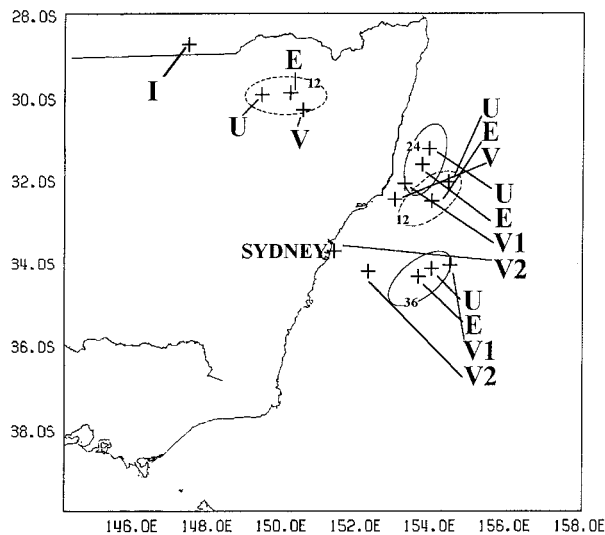


FIG. 6. Map of analysis and forecast domain showing low center position for initial analysis, **I**, at 0900 30 August 1996 and unperturbed, **U**, and ensemble mean, **E**, forecast SLP low center positions at 12, 24, and 36 h. Also shown are the verifying analysis positions **V**, based on observations for **I** and at 12 h, and **V1**, **V2** for 24 and 36 h.



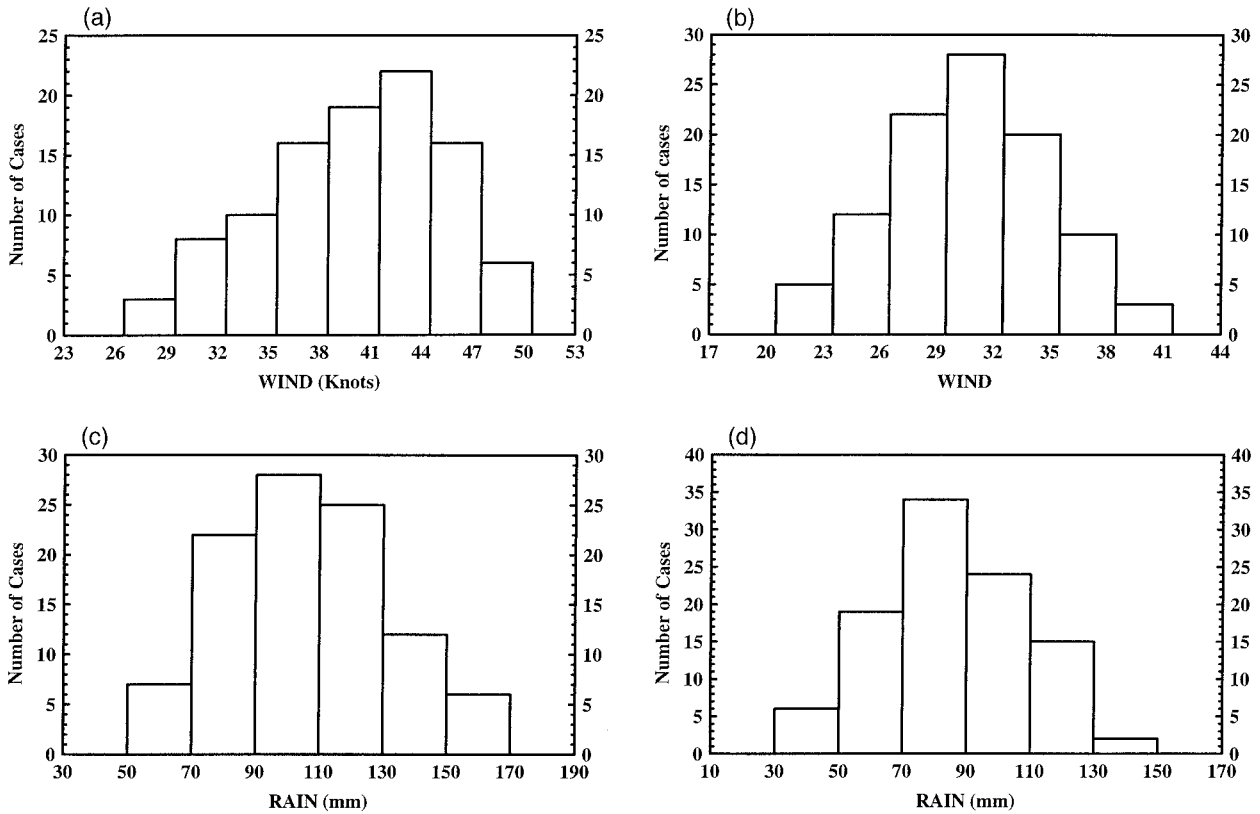


Fig. 7. (a) Frequency distribution of wind speed (kt) for the 100 ensemble forecasts over the 36-h forecast period at the model grid point closest to Sydney on the coast; (b) frequency distribution of wind speed (kt) for the 100 ensemble forecasts over the 36-h forecast period at the model grid point closest to Bankstown, a farther 30 km inland; (c) frequency distribution of rainfall amount (mm) for the 100 ensemble forecasts over the 36-h forecast period at the model grid point closest to Sydney on the coast; and (d) frequency distribution of rainfall amount (mm) for the 100 ensemble forecasts over the 36-h forecast period at the model grid point closest to Bankstown, a farther 30 km inland to the west of Sydney.

the coast over Sydney. The SLP forecast for **V1** at 2100 31 August (Fig. 5d) was remarkably good for a 36-h forecast compared with the observed analysis (Fig. 4d). The pressure drop of 19 hPa in 24 h at Sydney airport (Fig. 5e) signifies a bomb at Sydney's latitude but in developing the center of the low farther out to sea than the observed, there are differences in the detail of the pressure trace, in particular the period between midnight and 0500 where rapid intensification occurred right over the Sydney metropolitan area. The center **V2** was located on the northern outskirts of Sydney from a dense mesoscale network of surface observations there. Also, the HLAM unperturbed 36-h forecast winds (Fig. 5f)

predicted greater than 40 kt ( $20.6 \text{ m s}^{-1}$ ) over the coast in and near Sydney, similar to the observed, which can be considered useful guidance since there were maximum gusts of over 50 kt recorded, as mentioned in section 3.

*b. Ensemble forecasts*

Although the ensemble consisted of 100 forecasts perturbed from the initial conditions, there was little change for *this case* after about 30 model runs in the intensity and location of **V1**. These findings are in general agreement with studies carried out at operational centers including NCEP and ECMWF. The initial, **I**, and the unperturbed, **U**, and ensemble mean, **E**, low center posi-

TABLE 2. Columns 1 and 2 show the ensemble mean sustained wind speeds (kt) and standard deviations for the grid points closest to Sydney (on the coast) and Bankstown, a farther 30 km inland. These should be compared to the observed maximum sustained wind speeds for the observing stations of Sydney and Bankstown in column 3.

	Ensemble mean	Std dev	Obs max
Sydney	40	5	46
Bankstown	31	4.5	30

TABLE 3. As in Table 2 except for 24-h rainfall totals (mm).

	Ensemble mean	Std dev	Observed 24-h total rain to 0900 31 Aug
Sydney	106	26	127
Bankstown	86	23	85

tions for the 12-, 24-, and 36-h forecasts are shown in Fig. 6. Also shown are the verifying analysis positions, including **V1** and **V2**. The ellipses in Fig. 6 were drawn to cover all the 100 forecast position centers resulting from the perturbed initial conditions. Given that **E** lies between **V1** and **V2** at all lead times up to 36 h, the ensemble mean position provide enhanced guidance at all lead times. An interesting result emerged from this particular SREF application. The SLP center location ellipses showed very little change in time over the full 36-h period. This lack of increase in the spread of the forecasts is quite unusual in the authors previous experience. Over a reasonably large number of routine tropical and extratropical cyclone ensemble forecasts this generally has not been the case. Our only comment here is that this east coast low actually split into two centers and the ensemble mean was better positioned between these centers than the single unperturbed forecast, and therefore provided better guidance.

The ensemble mean wind forecast at 36 h (not shown) was over 40 kt ( $20.6 \text{ m s}^{-1}$ ) on the coast near Sydney, similar to the 36-h unperturbed forecast winds (Fig. 5f). Given that both the unperturbed and ensemble forecasts predicted winds greater than 40 kt, a forecast of land gales could have been made with confidence. This is confirmed by the frequency distribution of wind speed for the 100 ensemble forecasts at the model grid point closest to Sydney on the coast in Fig. 7a, which were indicating wind speeds of greater than 34 kt at the 36-h forecast period and about 70% were within one standard deviation ( $\pm 5$  kt) of the ensemble mean (40 kt). A further 30 km inland at the grid point closest to Bankstown (Fig. 7b) the unperturbed forecast wind speed and the ensemble mean were again similar, predicting maximum sustained wind speeds of over 30 kt ( $15 \text{ m s}^{-1}$ ). The SREF forecasts indicated that only 26% of the forecasts were above gale force. The ensemble mean, standard deviation, and the observed maximum wind speed, which are representative of Sydney on the coast and Bankstown, 30 km farther inland, are shown in Table 2. We have restricted our use of the probabilistic information provided by the SREF to probability ellipses, histograms, means, and standard deviations. This was a deliberate choice on our part as we are not yet sure of the value of other measures such as skewness, etc. As our familiarity with SREF increases, we might expect to glean more information from the ensembles.

Most of the rain fell within the 24 h to 0900 LST 31 August. For this period, the ensemble mean, standard deviation, and the observed rainfall amounts, which are representative of the two locations of Sydney and Bankstown, are shown in Table 3. Although the ensemble mean slightly underpredicted the rainfall amount, the forecast spread encompassed the observed 24-h total of 127 mm at Sydney (Fig. 7c). At Bankstown the ensemble mean rainfall amount was very close to the observed 24-h total of 85 mm (Fig. 7d). Again the forecast spread, that is, the standard deviation encompassed the

observed 24-h amount. There seems to be no obvious explanation for the smaller ensemble spread relative to the larger mean errors at the two stations other than to suggest that local influences, the fact that we are looking at only one case, and only two point sites are being examined might be responsible.

## 5. Discussion and conclusions

An explosive Australian east coast low event has been described in terms of a comparison between the unperturbed forecast and a Monte Carlo ensemble of meso-scale model forecasts at 15-km horizontal resolution covering the explosive development period. Overall, the unperturbed forecast was very good. The unperturbed SLP forecast for 12 h was excellent, showing development of the second center. Although the 24-h forecast did not predict the small center on the coast, the intensity of the system elsewhere was very encouraging. The 36-h forecast position of **V1** also was very good as were the intensity wind and precipitation forecasts. Given that the 75-km operational model did not predict land gales and that the forecasters also were not prepared on their available information to issue a forecast of land gales, it would have been desirable to have a measure of confidence in the forecast, hence the SREF study.

The ensemble 36-h SLP forecast low center, being located between **V1** and **V2**, would have provided enhanced guidance at the horizontal resolution of 15 km. Given the unperturbed forecast, plus confirmation from the 36-h ensemble mean forecast, a land gale warning could have been issued with a high level of confidence attached. From the guidance available at the time, ocean gales were forecast but not land gales. However, the significant probabilistic detail for wind and rainfall forecasts provided by the SREF would have been sufficient for the forecasters or end users to expect land gales to have occurred, and high 24-h precipitation totals of around 100 mm for the Sydney metropolitan area.

Finally, even though small-scale centers, such as **V2** in this case study, are not resolved at 15-km horizontal resolution in the model, additional significant probabilistic information was obtained from the ensemble forecasts for this example of an explosive Australian east coast cyclone.

*Acknowledgments.* The authors would like to express their appreciation to an anonymous reviewer who helped considerably in improving the manuscript. One of the authors (LML) was partially supported in this work by ONR Grant N00014-94-1-0556.

## REFERENCES

- Brooks, H. E., M. S. Tracton, D. J. Stensrud, G. DiMego, and Z. Toth, 1995: Short-range ensemble forecasting: Report from a workshop, 25–27 July 1994. *Bull. Amer. Meteor. Soc.*, **76**, 1617–1624.

- Daley, R., 1991: *Atmospheric Data Analysis*. Cambridge University Press, 457 pp.
- Doswell, C. A., III, 1996: Severe weather warning services: Responsibilities to the public. Preprints, *Fifth Australian Severe Thunderstorm Conf.*, Avoca Beach, New South Wales, Australia, Bureau of Meteorology, 205–209. [Available from Bureau of Meteorology, P.O. Box 1289K, Melbourne, Australia.]
- Golding, B. W., and L. M. Leslie, 1993: The impact of resolution and formulation on model simulations of an east coast low. *Aust. Meteor. Mag.*, **42**, 105–116.
- Hess, G. D., 1990: Numerical simulation of the August 1986 heavy rainfall event in the Sydney area. *J. Geophys. Res.*, **95** (D3), 2073–2082.
- Hopkins, L. C., and G. J. Holland, 1997: Australian heavy-rain days and associated east coast cyclones: 1958–92. *J. Climate*, **10**, 621–635.
- Leith, C. E., 1974: Theoretical skill of Monte Carlo forecasts. *Mon. Wea. Rev.*, **102**, 409–418.
- Leslie, L. M., and R. J. Purser, 1995: Three-dimensional mass-conserving semi-Lagrangian scheme employing forward trajectories. *Mon. Wea. Rev.*, **123**, 2551–2556.
- , G. J. Holland, and A. Lynch, 1987: Australian east-coast cyclones. Part II: Numerical modeling study. *Mon. Wea. Rev.*, **115**, 3037–3053.
- McInnes, K. L., and G. D. Hess, 1992: Modifications to the Australian region limited area model and their impact on an east coast low event. *Aust. Meteor. Mag.*, **40**, 21–31.
- Molteni, F., R. Buizza, T. N. Palmer, and T. Petroliaigis, 1996: The ECMWF ensemble system: Methodology and validation. *Quart. J. Roy. Meteor. Soc.*, **122**, 73–120.
- Mullen, S. L., and D. P. Baumhefner, 1989: The impact of initial condition uncertainty on numerical simulations of large-scale explosive cyclogenesis. *Mon. Wea. Rev.*, **117**, 2800–2821.
- , and ———, 1994: Monte Carlo simulations of explosive cyclogenesis. *Mon. Wea. Rev.*, **122**, 1548–1567.
- Puri, K., G. Dietachmayer, G. Mills, N. Davidson, R. Bowen, L. Logan, and L. Leslie, 1996: The new BMRC regional assimilation and prediction system. BMRC Research Rep. 52, 168 pp. [Available from Bureau of Meteorology, P.O. Box 1289K, Melbourne, Australia.]
- Sanders, F., and J. R. Gyakum, 1980: Synoptic-dynamic climatology of the “bomb.” *Mon. Wea. Rev.*, **108**, 1589–1606.
- Toth, Z., and E. Kalnay, 1993: Ensemble forecasting at NMC: The generation of perturbations. *Bull. Amer. Meteor. Soc.*, **74**, 2317–2330.
- Warner, T. T., R. A. Peterson, and R. E. Treadon, 1997: A tutorial on lateral boundary conditions as a basic and potentially serious limitation to regional numerical weather prediction. *Bull. Amer. Meteor. Soc.*, **78**, 2599–2618.